



OPEN Matched three-dimensional organoids and two-dimensional cell lines of melanoma brain metastases mirror response to targeted molecular therapy

William H. Hicks^{1,2}, Lauren C. Gattie^{1,2}, Mohamad El Shami^{1,2}, Jeffrey I. Traylor^{3,4}, Diwakar Davar², Yana G. Najjar², Timothy E. Richardson⁵, Samuel K. McBrayer^{3,6,7} & Kalil G. Abdullah^{1,2,8}✉

Despite advances in the treatment paradigm for patients with metastatic melanoma, melanoma brain metastasis (MBM) continues to represent a significant treatment challenge. The study of MBM is limited, in part, by shortcomings in existing preclinical models. Surgically explanted Organoids (SXOs) are *ex vivo*, three-dimensional cultures prepared from primary tissue samples with minimal processing that recapitulate genotypic and phenotypic features of parent tumors without an artificial extracellular scaffold. MBM SXOs were created by a novel protocol incorporating techniques for establishing glioma and cutaneous melanoma organoids. A BRAF^{V600K}-mutant and BRAF-wildtype MBM sample were collected directly from the operating room. Organoids were cultured in an optimized culture medium without an artificial extracellular scaffold. Concurrently, matched patient-derived cell lines were created. Organoid growth was observed within 3–4 weeks, and MBM SXOs retained histological features of the parent tissue, including pleomorphic epithelioid cells with abundant cytoplasm, large nuclei, focal melanin accumulation, and strong SOX10 positivity. After sufficient growth, organoids could be manually parcellated to increase the number of replicates. Matched SXOs and cell lines demonstrated sensitivity to BRAF and MEK inhibitors. Further study using SXOs may improve the translational relevance of preclinical studies and enable the study of the metastatic melanoma tumor microenvironment.

Keywords Metastatic melanoma, Organoids, Melanoma brain metastasis, Preclinical cancer model

Melanoma brain metastasis (MBM) represents a significant treatment challenge¹. While combinatorial systemic targeted therapy in some subtypes has shown reasonable control rates in extracranial tumor burden, this treatment regimen has produced a less durable response in progressive central nervous system (CNS) disease^{2–4}. The recent CheckMate 204 trial demonstrated concordant intracranial and extracranial benefits with combined immune checkpoint inhibitors; however, further study is needed to assess optimal therapy regimens, particularly in symptomatic MBM^{5,6}. The decreased effectiveness of systemic targeted therapy to brain metastases has been thought to be related to poor blood-brain barrier penetration, the unique brain-tumor interface, and immune considerations of the brain-tumor immune microenvironment (TIME)^{7–9}. While these interactions are critical to

¹Department of Neurological Surgery, University of Pittsburgh, 200 Lothrop St, Pittsburgh, PA 15213, USA. ²Hillman Comprehensive Cancer Center, University of Pittsburgh Medical Center, 5115 Centre Ave, Pittsburgh, PA 15232, USA. ³Children's Medical Center Research Institute, University of Texas Southwestern Medical Center, 6000 Harry Hines Blvd, Dallas, TX 75235, USA. ⁴Department of Neurological Surgery, University of Texas Southwestern Medical Center, 5303 Harry Hines Blvd, Dallas, TX 75390, USA. ⁵Department of Pathology, Molecular and Cell-Based Medicine, Icahn School of Medicine at Mount Sinai, 1468 Madison Ave, New York, NY 10029, USA. ⁶Department of Pediatrics, University of Texas Southwestern Medical Center, Dallas, TX 75390, USA. ⁷Simmons Comprehensive Cancer Center, University of Texas Southwestern Medical Center, Dallas, TX 75390, USA. ⁸Department of Neurological Surgery, University of Pittsburgh Medical Center Hillman Cancer Center, 5150 Centre Avenue, Suite 430, Pittsburgh, PA 15232, USA. ✉email: abdullahkg@upmc.edu

investigate, existing model systems have limited our ability to evaluate the response of MBM to immunotherapy in the laboratory.

Two-dimensional melanoma cell lines are essential for high-throughput, in vitro drug sensitivity studies; however, these systems do not reflect the complex cellular heterogeneity of human metastatic brain tumors¹⁰. Patient-derived xenograft models enable studies of drug responses in a relevant cellular milieu but are intrinsically low-throughput, carry long latency times, and the strains used for xenotransplantation limit evaluation of the TIME^{11,12}. Patient-derived three-dimensional organoids have emerged as an attractive system for modeling the heterogeneous microenvironment of advanced cancers¹³. Traditional approaches to organoid modeling have used isogenic cell lines or enzymatically dissociated patient-derived tumor samples¹⁴. However, these techniques often simultaneously rely on the supplementation of exogenous growth factors and sample engrafting in an artificial extracellular matrix (ECM), such as Matrigel, Geltrex, or collagen gel scaffolds^{13,15}. Additionally, their clonal nature limits elements of the TIME that may drive treatment response or resistance.

Recently, our group demonstrated an optimized and efficient method to produce Surgically eXplanted Organoids (SXOs) of low-grade glioma from resected tumor samples that faithfully maintain the histology, genetics, and cellular composition of the parent tissue¹⁶. These SXOs can be established at an almost 90% success rate from both low- and high-grade gliomas and model the differential sensitivities to drugs that selectively target *IDH*-mutant gliomas^{16,17}. Notably, this approach to producing SXOs does not require an artificial ECM, thus providing a more faithful and physiologically relevant ex vivo model system. Recently, a minimally processed technique was used to generate patient-derived organoids from cutaneous melanoma samples^{18,19}. While this technique has clear advantages over protocols that dissociate tissues to single or near-single cell suspensions, it requires engraftment into an artificial ECM, is derived from a clonal progenitor cell, and exists in a system that lacks crucial elements of the TIME. To create an SXO model of MBM, we sought to adapt these techniques to incorporate elements of the glioma SXO model approach with variations in media concentrations to facilitate the growth of these metastatic lesions^{16,18,19}.

Herein, we detail the creation of three-dimensional, scaffold-free SXOs of MBM directly from primary patient tumor samples (Fig. 1). Additionally, we show that the MBM SXOs retain the histopathologic characteristics of the parent tissue and mirror predicted sensitivities to targeted therapeutics. To our knowledge, this is the first report of a scaffold-free organoid model of melanoma and is the first organoid model of MBM. These findings suggest that MBM SXOs may serve as a novel, physiologically relevant model system for therapeutic screening and translational studies of this disease.

Materials and methods

Human specimens

All patient tissue and blood samples were collected following ethical and technical guidelines on the use of human samples for biomedical research at the University of Pittsburgh and the University of Pittsburgh Medical Center after informed consent was obtained from patients under the Institutional Review Board Protocol (19080321). The study was conducted according to the principles of the Declaration of Helsinki.

Organoid creation and culture in melanoma complete media

Tumor tissue was collected and processed as previously described¹⁶. Freshly resected tumor tissue was collected directly from the operating room, placed in ice-cold Hibernate A (BrainBits HA), and returned to the lab for further processing within 30 min of resection. Tumor pieces were submerged in RBC Lysis Buffer (ThermoFisher 00433357) and incubated on a rocker at room temperature for 10 min. Then, the RBC Lysis Buffer was aspirated, and the tumor pieces were washed with Hibernate A solution containing Glutamax (2 mM, ThermoFisher 35050061), Penicillin/Streptomycin (100 U/mL and 100 µg/mL, respectively, ThermoFisher 15140122), and Amphotericin B (0.25 µg/mL, Gemini Bio-Products 400104). Tissues were transferred to a sterile culture dish, manually parcellated using a 1.0 mm biopsy punch (ThermoFisher 12460401), and suspended in 1 mL of Melanoma Organoid Complete Media (formula below), with one organoid plated per well of a 24-well flat-bottom ultra-low adherence plate (Corning 3473)¹⁸. Plates were incubated in a humidified incubator at 37 °C, 5% CO₂, and 21% O₂ under continuous orbital rotation at 120 rpm. SXO media was replaced every other day, with 75–90% of media being replaced. Melanoma Organoid Complete Media formula¹⁸: 250 mL DMEM (Sigma D6429), 125 mL Nutrient Mixture Ham's F12 (Sigma N4888), 125 mL MCDB 105 Medium (Cell Applications 117–500), 50 mL fetal bovine serum (Gibco 26140079), 5 mL Glutamax (2 mM, ThermoFisher 35050061), 5 mL Penicillin/Streptomycin (100 U/mL and 100 µg/mL, respectively, ThermoFisher 15140122), 10 mL B-27 supplement (Gibco 17504044), 1 mL Normocin (Invivogen ant-nr-1). Melanoma Organoid Complete Media stocks were used up to 1 month after preparation. Organoids were suitable for evaluation and downstream assays after two to four weeks as assessed by stability in organoid size, growth in culture, and histopathologic examination at predetermined intervals. As a standard practice, SXOs were cultured for at least four weeks post-explantation before any experiments were undertaken. Organoid size was inspected weekly and manually parcellated to a diameter of less than one millimeter to avoid limits in nutrient diffusion and central necrosis.

Human melanoma brain metastasis cell generation

The MBM739 cell line was generated from a human melanoma brain metastasis (UPMC739). The Human Tumor Dissociation Kit (Miltenyi Biotec 130095929) was used per the manufacturer's protocol to generate a single-cell suspension from the tumor sample. After dissociation, cells were cultured in DMEM (Sigma D6546) supplemented with 10% fetal bovine serum, 5 mL Glutamax (2 mM, ThermoFisher 35050061), and 5 mL Penicillin/Streptomycin (100 U/mL and 100 µg/mL, respectively, ThermoFisher 15140122) at 37 °C, 5% CO₂, and 21% O₂. Cells were cultured in adherent culture dishes and passaged 1–2 times per week with 0.25% trypsin.

Creation of a Surgically eXplanted Organoid (SXO) Model of Metastatic Melanoma to the Brain

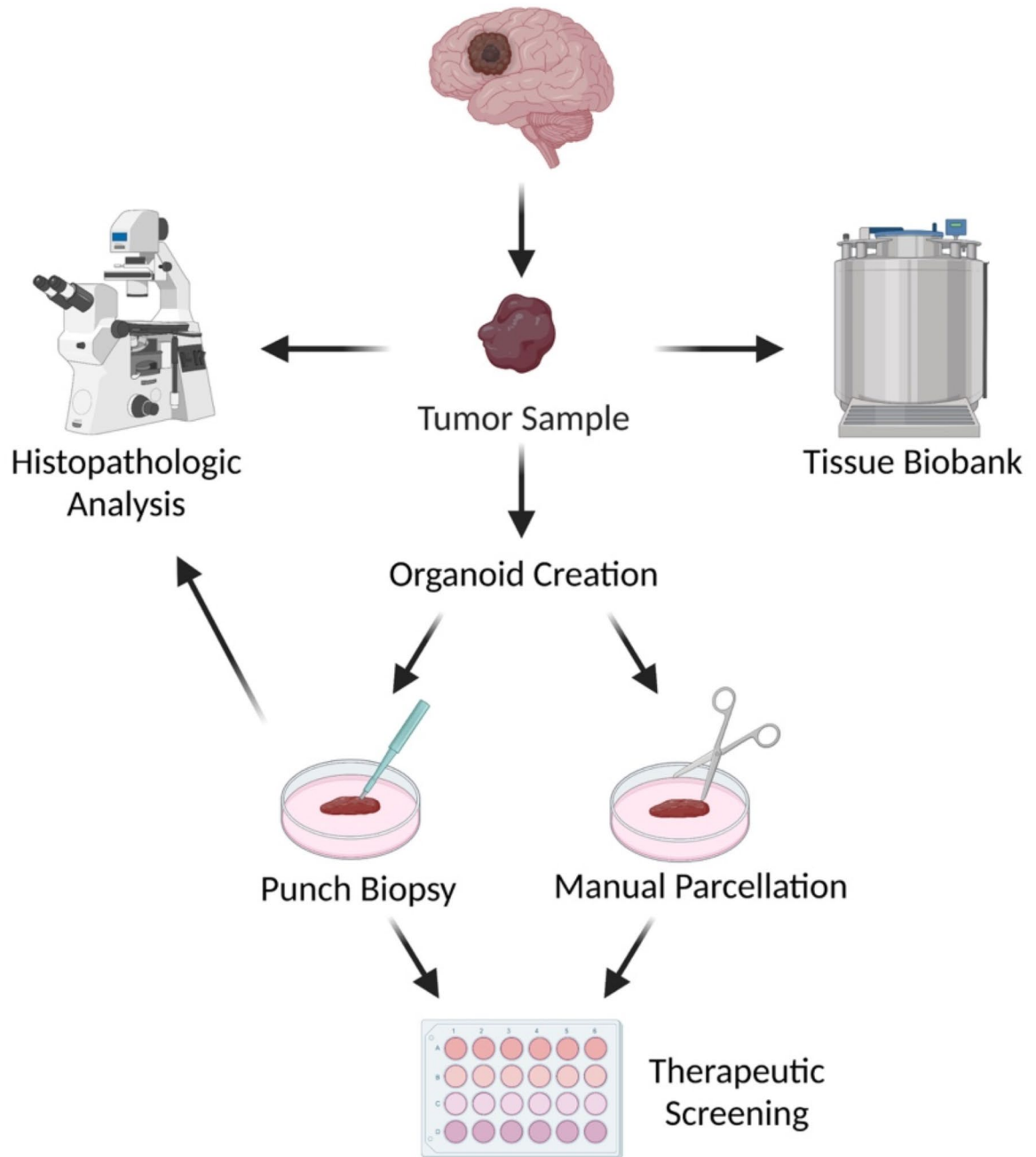


Fig. 1. Overview of the creation of Surgically Explanted Organoids (SXOs) of Melanoma Brain Metastases (MBM). Tissue samples of MBM were collected from the operating room, manually parcellated, and cultured in optimized Melanoma Organoid Complete Media. SXOs were suitable for downstream experiments two to four weeks after explant and were cultured for at least four weeks before use in downstream experiments. Additionally, primary tissue and derivative organoids were cryopreserved for future analyses. Organoids were randomized to all treatment groups. Figure created with BioRender.

Histopathology and immunohistochemistry

SXOs and primary tissue samples were fixed in 10% formalin for 1 h and then washed and resuspended in 70% ethanol. After the alcohol wash, SXOs were transferred to the cap of a 1.5 mL cryotube, resuspended in 0.5% agarose gel, and allowed to solidify overnight at 4 °C. The following morning, the agarose-organoid molds were transferred to a cassette, dehydrated in 10% formalin, 70% ethanol three times for 30 min, 90% ethanol twice for 30 min, 100% ethanol three times for 30 min, xylene three times for 20 min, and embedded in paraffin. Paraffin blocks were sectioned at 4- μ m thickness. For hematoxylin and eosin (H&E) staining, slides were deparaffinized in xylene (9 min), 100% ethanol (3 min), 95% ethanol (1 min), and stained with hematoxylin (20 s). Slides were rinsed in water, soaked in clarifier (40 s), washed in water, and then bluing agent (20 s). Slides were then rinsed, stained with eosin (20 s), followed by serial incubation in 100% ethanol (3 min) and xylene (3 min), and then mounted for microscopic examination. Immunohistochemistry (IHC) staining was performed via the Cell Signaling Technology citrate unmasking protocol. Antibodies used included an anti-human Sox10 rabbit antibody (1:100, Abcam ab227680) and an anti-human Gp100 mouse antibody (1:100, Abcam ab732, clone HMB45).

Cell viability assay

Cell viability assays were performed by seeding 5,000 cells/well in a 96-well opaque walled plate. Replicates were then treated with the BRAF inhibitor, dabrafenib (Sellekchem S2807), MEK inhibitor, trametinib (Sellekchem S2673), or combined treatment. The CellTiter-Glo Luminescent Viability Assay (Promega G7571) was used to measure cell viability at 24, 48, and 72 h following the manufacturer's protocol. Luminescence was measured using the Tecan M1000 Pro Microplate Reader. The SynergyFinder+ web application (06.3.2024-R-3.10.3, synergyfinder.org) was used to evaluate the relationship of combined dabrafenib and trametinib treatment and assess for synergy using the HSA, Loewe, and Bliss methods²⁰.

Organoid viability assay

Organoids were treated with the respective drug diluted in Melanoma Complete Media. At the desired time point, SXO viability was assessed using the ReadyProbe Cell Viability Kit (Invitrogen R37610). Briefly, treated organoids were removed from the incubator, approximately 90% of the media was removed, and 500 μ L fresh media was added. Then, 20 μ L of the NucBlue/Hoechst and 20 μ L of the propidium iodide (PI) dye were added. Organoids were then returned to the incubator under orbital rotation for 20 min. Fluorescent live cell imaging of the organoids was then captured on the Nikon CrestOptics X-Light V3 spinning disk confocal microscope at 40X magnification. An executable application was run within the Nikon NIS-Elements software to denoise and generate a three-dimensional maximal projection of the organoid from which the individual counts of Hoechst-positive and PI-positive cells could be quantified. Organoid viability was quantified using the Nikon NIS-Elements software to generate the percent viability of live cells (Hoechst positive) relative to dead cells (Hoechst plus PI). Prior correlation of cellularity and viability between live cell imaging and traditional histopathology establishes the utility of this assay in assessing treatment response²¹.

Statistical analysis

SXOs were allocated to experiments randomly. All statistical tests were two-sided, where applicable. Student's *t*-tests were used to assess the statistical significance of differences between groups. Statistical analyses were performed with GraphPad Prism (9.5.1.528, GraphPad Software, LLC) and included both descriptive statistics and tests of statistical significance. All data are plotted as mean \pm standard deviation. For all tests, *p*-values less than 0.05 were considered statistically significant.

Results

We created two unique models of MBM. Patient 1 (UPMC739) was a 54-year-old male with a 5-year history of BRAF^{V600K}-mutant oligometastatic melanoma to the bowel and kidney who had undergone multiple extracranial resections as well as nivolumab and encorafenib/binimetinib treatments following multiple episodes of disease progression. He presented with new symptomatic multifocal brain metastases and underwent resection of a symptomatic left temporal lobe mass (Fig. 2a). Patient 2 (UPMC754) was a 62-year-old male with a 2-year history of BRAF-wildtype metastatic melanoma to the lungs who had undergone prior resection and treatment with nivolumab and duvelisib. He underwent resection of a symptomatic new large left cerebellar mass in the setting of multifocal MBM (Fig. 2b). Clinical pathologies were consistent with metastatic melanoma, denoted by epithelioid tumor cells with amphophilic cytoplasm, severe pleomorphism, prominent nucleoli, and variable (UPMC739) or absent (UPMC754) pigment staining. The tumor cells were positive for SOX10, gp100, and patchy MelanA by immunohistochemistry (IHC). From each tumor sample, we successfully generated SXOs and cultured them in Melanoma Organoid Complete Media¹⁸ for four weeks before treatment studies. In parallel, we established a two-dimensional cell line, MBM739, from the primary tissue of UPMC739 using an available human tumor dissociation protocol. Cells were passaged weekly until capable of sufficient proliferative ability for downstream assays.

MBM SXOs preserve histologic features of the parent tumor

We assessed SXO cytoarchitecture and viability with assistance from a board-certified neuropathologist (T.E.R.). We found that the SXO models recapitulated the histopathologic features of the parent tumor on hematoxylin and eosin (H&E) staining, with epithelioid cells and pleomorphic nuclei (Fig. 3). On visual inspection, the SXOs from UPMC739 were melanotic in appearance. In contrast, the SXOs from UPMC754 were tan and amelanotic, consistent with the degree of pigmentation present in the primary tumor histology. These pigmentation patterns were retained in culture, both grossly and on histopathology. Additionally, the IHC of both SXO models

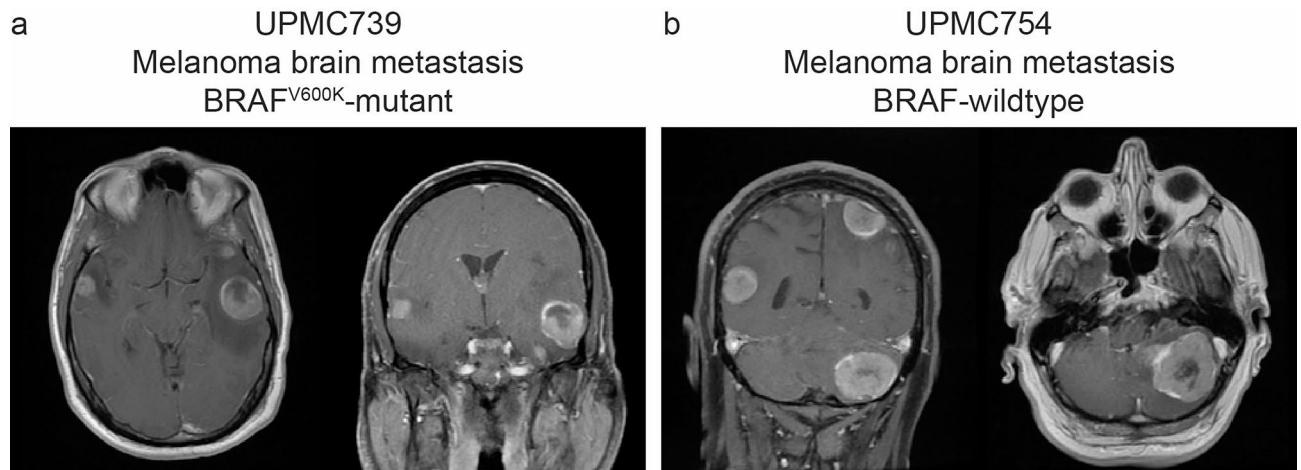


Fig. 2. Preoperative axial and coronal T1 post-contrast magnetic resonance imaging (MRI) of (a) Patient 1 (UPMC739) revealing a large left temporal lobe melanoma metastasis, and (b) Patient 2 (UPMC754) revealing a large left cerebellar melanoma metastasis.

demonstrated diffuse positivity for SOX10, a reliable marker of multiple histologic subtypes of malignant melanoma²², and UPMC739 was positive for gp100.

Matched patient-derived cell line and surgically eXplanted organoids (SXOs) demonstrated sensitivity to dabrafenib and trametinib

To evaluate whether our patient-derived MBM models demonstrate predicted sensitivities to targeted molecular therapies, we treated the MBM739 cell line with dabrafenib (BRAF inhibitor), trametinib (MEK inhibitor), or combined BRAF-MEK inhibition with both agents (Fig. 4a). The 48-hour dose-response curves for each agent guided the selection of treatment concentrations for the SXOs (Fig. 5a-b). The estimation of synergy between the two treatments by the HSA, Loewe, and Bliss models showed additive effects of combined BRAF and MEK inhibition (HSA Score = 3.5, Loewe score = 8.49, and Bliss Score of -0.038) in the MBM739 cell line after 24 h of treatment (Fig. 5c-f). We then administered the effective doses of each treatment to the MBM SXOs for 48 h. We evaluated their response using an established method for live cell fluorescence imaging microscopy²¹. There was an appreciable increase in the PI signal with monotherapy treatment and a significant decrease in the organoid viability with dual-targeted molecular therapy (Fig. 4b), with quantitative Live-Dead analysis of the organoids treated with combined BRAF-MEK inhibition resulting in a statistically significant decrease in MBM SXO viability (Fig. 4c).

Discussion

Here, we detail a protocol for a novel preclinical model of MBM and the first known scaffold-free organoid model of melanoma. Further, we have shown the ability to screen the sensitivity of MBM SXOs to targeted therapeutic agents. The generation of this model answers a prior unmet need for a physiologically relevant preclinical system to guide translational studies of MBM.

Melanoma is highly aggressive and carries a significant mortality rate due to its rapid proliferation, early and recurrent metastatic disease propensity, particularly to the CNS, and intratumor heterogeneity^{23,24}. While combination targeted molecular therapy and immunotherapy have shown success in treating extracranial disease burden, the degree of disease response for MBM has been more limited. While a recent study demonstrated that treatment of asymptomatic MBM with nivolumab plus ipilimumab (Checkmate 204, open-label phase 2 results) was feasible, there remain critical subsets of patients who either develop symptomatic MBM or who progress despite combinatorial therapy⁶.

Alternatively, the outcomes in MBM may be attributable to the paucity of relevant model systems that faithfully and reliably model human metastatic melanoma to the brain²⁵. Two-dimensional cell lines frequently lack intratumoral heterogeneity, traditional xenograft models limit the study of the TIME, and genetically engineered mouse models often produce oligoclonal tumors compared to the polyclonal heterogeneity seen in human melanoma, particularly in the case of metastatic disease²⁵. Thus, the protocol outlined here may bridge a translational gap by providing a preclinical MBM model that is temporally related to the primary human tumor, has minimal ex vivo processing, retains the key histopathologic features of the primary tumor, and mirrors predicted drug sensitivities of the primary tumor based on known molecular profiles.

A downstream application of this model system is in performing preclinical therapeutic screening. In addition to being useful in testing sensitivity to targeted molecular therapies, as seen in the current study and our prior studies targeting *IDH*-mutant glioma^{16,17}, we have shown that SXOs provide reliable treatment responses in multi-modality evaluations of targeted therapeutics^{26,27}. Our study demonstrated the utility of this model system in assessing treatment response to targeted agents against upregulated cell signaling pathways in BRAF-mutant MBM^{28–30}. Patient-derived organoids have been used to perform comprehensive drug screens in extracranial

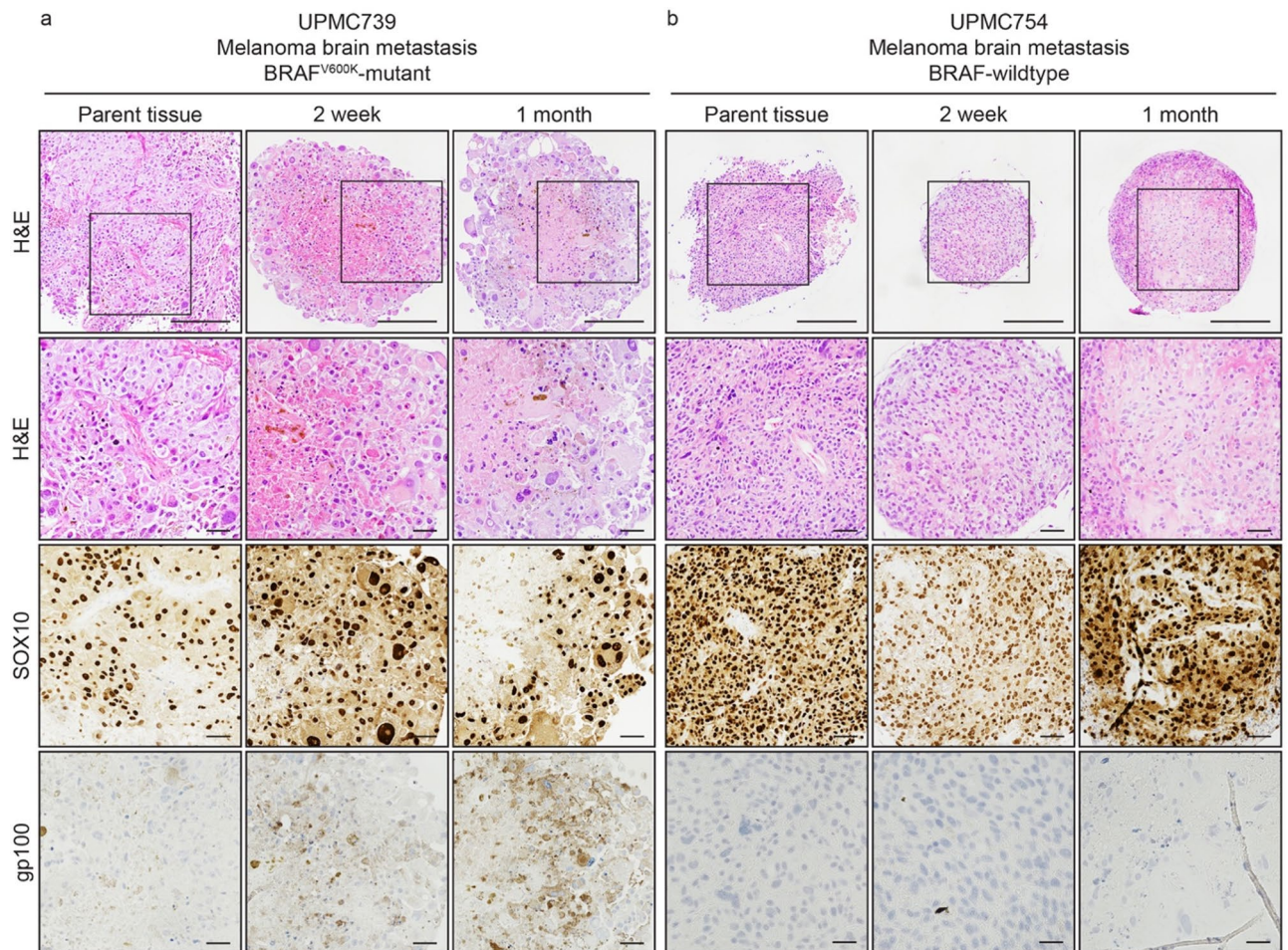


Fig. 3. Surgically eXplanted Organoids (SXOs) of melanoma brain metastases retain the cellularity and histopathologic characteristics of the parent tissue. Explanted tissue and organoids were formalin-fixed and paraffin-embedded for histopathologic analysis at routine intervals, including at the time of surgery, two weeks post-resection, and one month post-resection. H&E slides demonstrate similar histological characteristics of SXOs to the parent tissue, including pleomorphic epithelioid cells with abundant cytoplasm, large nuclei, and focal (UPMC739) or absent (UPMC754) melanin accumulation. Immunohistochemistry shows that primary tissue and SXOs are diffusely SOX10 positive and gp100 positive (UPMC739). Scale bar = 125 μm and insets = 50 μm .

platforms for breast, liver, and colorectal cancers, among others^{13,31,32}. Notably, the minimally processed SXO model can be produced in a clinically relevant timeline³³. As with the results from our prior studies, the cultured MBM SXOs are suitable for use within 2–4 weeks of creation, in line with the timing for postoperative recovery, histopathologic analysis of biopsied or resected tissue, and genomic sequencing profiles to result. With clinical practice for most hematologic and solid malignancies centered around individual cancer's genetic profile, a comprehensive preclinical drug screen of the patient's tumor would be an additional tool to guide personalized oncology³⁴.

Beyond their initial applications in translational therapeutic screenings, SXOs offer a novel avenue to understand melanoma biology. Glioma SXOs have demonstrated preservation of the tumor, non-immune, and infiltrating immune cells, enabling the study of the tumor microenvironment^{16,35}. Particularly when studying melanoma, where systemic immunotherapy has shown significant efficacy, a model system to study these interactions *ex vivo* is critical. A recent study by Ou et al. created a scaffolded organoid model of extracranial malignant melanoma. They found they could successfully model the immunosuppressive microenvironment and sensitivity to immune checkpoint blockade *in vivo*³⁶. Additionally, we have recently shown the ability to perform stable isotope tracing of glioma SXOs, providing another unique avenue to study tumor metabolism in metastatic cancer of the brain³⁷.

Limitations

We acknowledge that our study is not without limitations. All replicates were derived from two patients and may not fully represent the generalizability of this protocol. Further, the sensitivity of the BRAF^{V600K}-mutant MBM SXO to dabrafenib and trametinib may have been confounded by prior exposure to encorafenib and binimetinib,

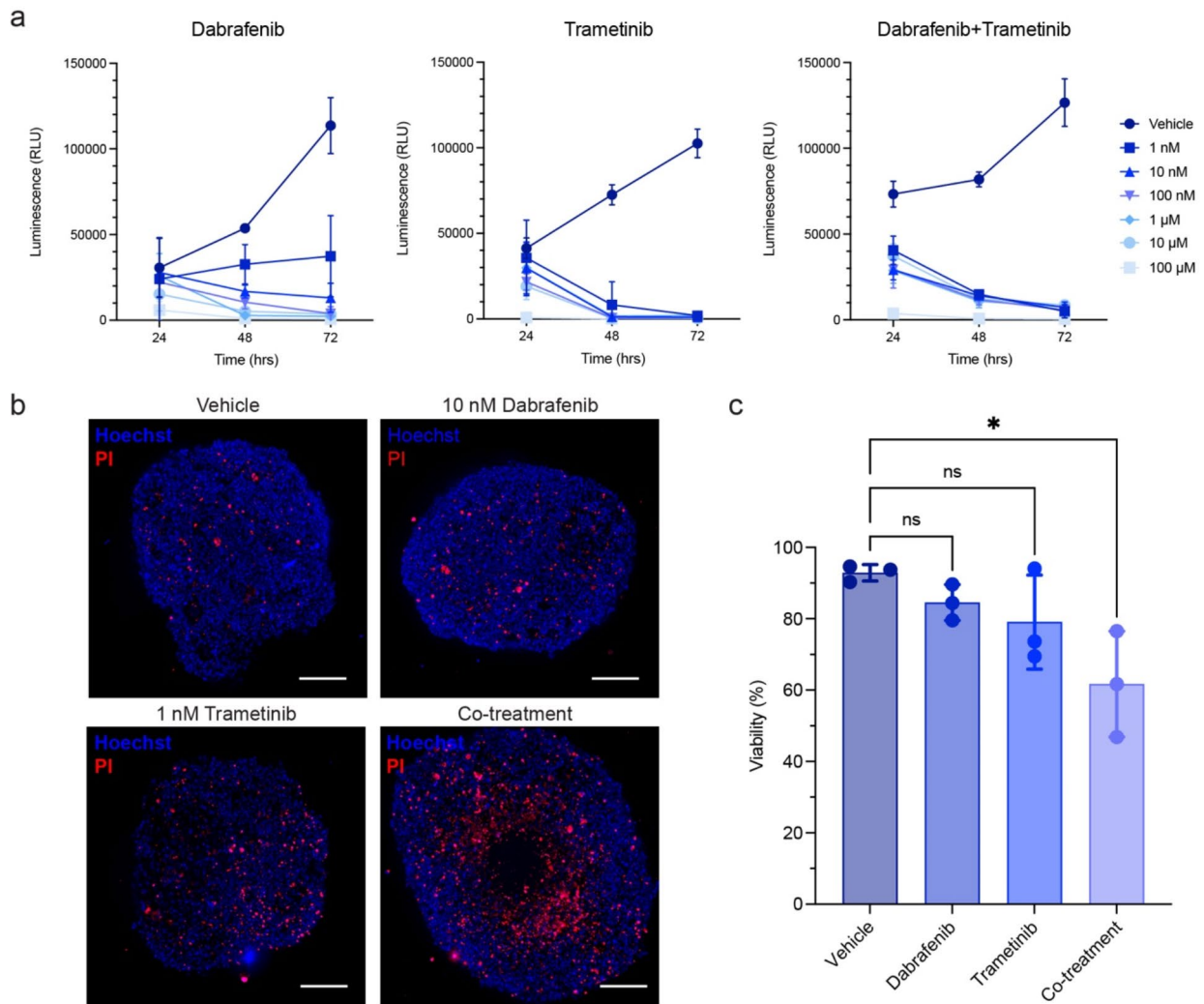


Fig. 4. Matched patient-derived cell line and surgically explanted organoids (SXOs) of BRAF^{V600K}-mutant metastatic melanoma to the brain demonstrate sensitivity to combined targeted therapy agents, dabrafenib and trametinib. (a) Decreased viability of the two-dimensional cell line MBM739, derived from UPMC739, in response to increasing dabrafenib, trametinib, or combined agents as assessed by the Cell-Titer Glo assay. (b) Fluorescent-based viability assay of MBM SXOs revealed maintenance of organoid structural integrity with increased cell death after 48 h of treatment. (c) Quantification of SXO viability demonstrates the mild effect of monotherapy and an additive effect with dual-targeted therapy. Data are presented as means \pm standard deviation; ns = not significant; * $p < 0.05$. $n = 3$ technical replicates for all treatment groups. Scale bar = 250 μ m.

an alternative BRAF/MEK inhibitor combination. The number of SXO replicates is limited ($n = 3$ for histology and $n = 3$ for drug treatments). It should be noted that the generation and maintenance of SXOs is contingent on precise attention to culture media, and our study marries the culture needs of rapidly-derived tissue explants and melanoma-specific media, which was critical in the generation of these models. This is further supported by prior organoid studies in which different culture media conditions with the appropriate growth factors are required to create and propagate breast, lung, and brain cancer organoids^{13,16,35}. Additionally, an expeditious relay between the operating room and the laboratory is essential, as these explants have shown high sensitivity to delays in culture conditions.

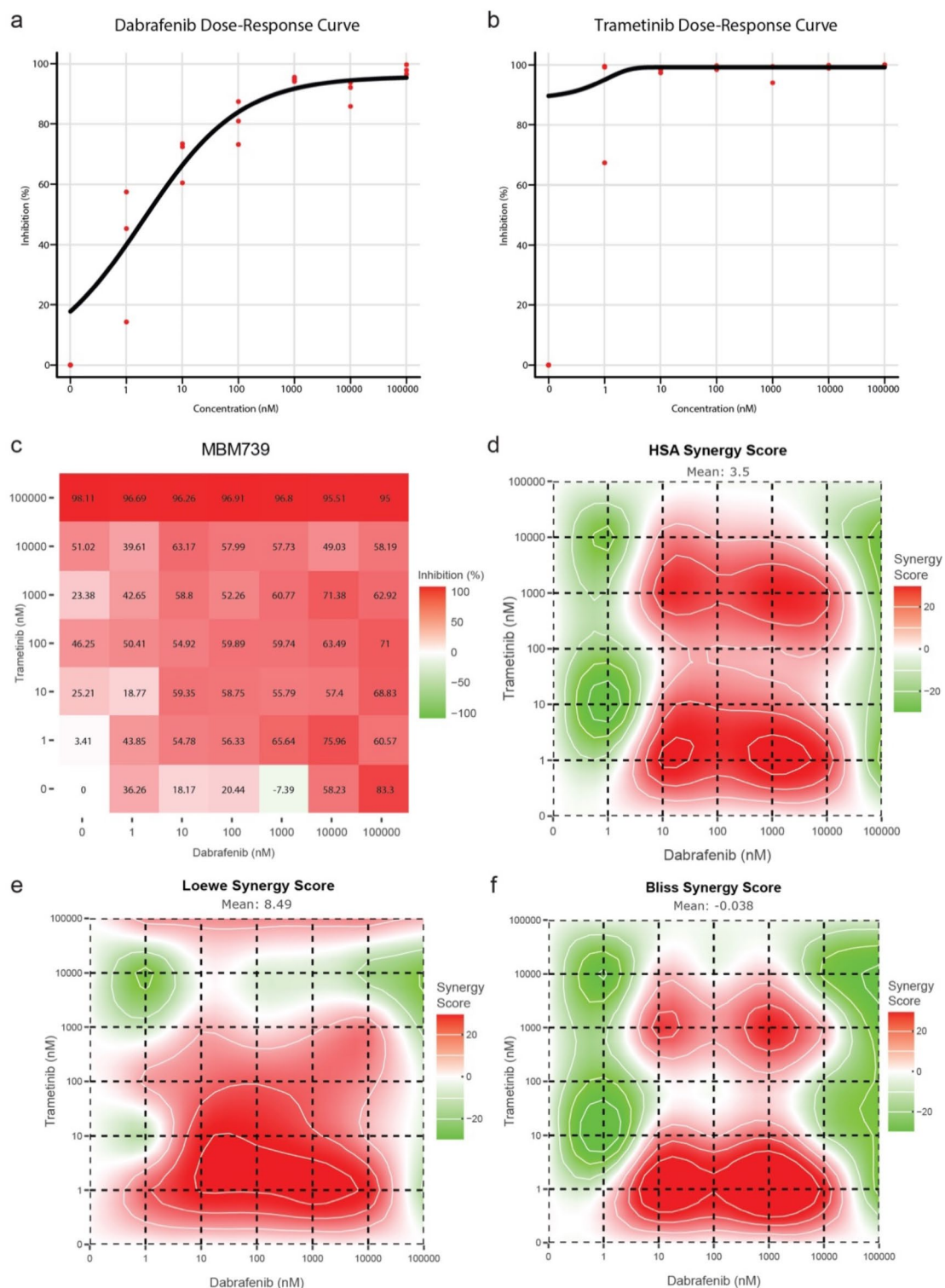


Fig. 5. Synergy analysis of treatment in melanoma brain metastasis cell line MBM739 using SynergyFinder+. (a–b) Dose-response curves of dabrafenib and trametinib at 48 h. (c) Dose-response matrix of monotherapy and combined therapy after 24 h. (d–f) HSA Synergy Score, Loewe Synergy Score, and Bliss Synergy Score maps demonstrating additive effects of combined BRAF + MEK inhibition after 24 h. $n = 3$ technical replicates for all treatment groups.

Data availability

Data is provided within the manuscript. Requests for information, resources, and reagents should be directed to and will be fulfilled by the Lead Contact, William H. Hicks (william.h.hicks@outlook.com). Additional histopathology images will be shared by the lead contact upon request. Any additional information required to reanalyze the data reported in this paper is available from the lead contact upon request.

Received: 18 March 2024; Accepted: 15 October 2024

Published online: 22 October 2024

References

- Gutzmer, R. et al. Melanoma brain metastases – interdisciplinary management recommendations 2020. *Cancer Treat. Rev.* **89**, 102083. <https://doi.org/10.1016/j.ctrv.2020.102083> (2020).
- Rishi, A. & Yu, H. H. M. Current treatment of Melanoma Brain Metastasis. *Curr. Treat. Options Oncol.* **21**, 45. <https://doi.org/10.1007/s11864-020-00733-z> (2020).
- Bander, E. D. et al. Melanoma brain metastasis presentation, treatment, and outcomes in the age of targeted and immunotherapies. *Cancer.* **127**, 2062–2073. <https://doi.org/10.1002/cncr.33459> (2021).
- Davies, M. A. et al. Dabrafenib plus Trametinib in patients with BRAF(V600)-mutant melanoma brain metastases (COMBI-MB): a multicentre, multicohort, open-label, phase 2 trial. *Lancet Oncol.* **18**, 863–873. [https://doi.org/10.1016/s1470-2045\(17\)30429-1](https://doi.org/10.1016/s1470-2045(17)30429-1) (2017).
- Tawbi, H. A. et al. Combined Nivolumab and Ipilimumab in Melanoma Metastatic to the brain. *N Engl. J. Med.* **379**, 722–730. <https://doi.org/10.1056/NEJMoa1805453> (2018).
- Tawbi, H. A. et al. Long-term outcomes of patients with active melanoma brain metastases treated with combination nivolumab plus ipilimumab (CheckMate 204): final results of an open-label, multicentre, phase 2 study. *Lancet Oncol.* **22**, 1692–1704. [https://doi.org/10.1016/S1470-2045\(21\)00545-3](https://doi.org/10.1016/S1470-2045(21)00545-3) (2021).
- Murrell, J. & Board, R. The use of systemic therapies for the treatment of brain metastases in metastatic melanoma: opportunities and unanswered questions. *Cancer Treat. Rev.* **39**, 833–838. <https://doi.org/10.1016/j.ctrv.2013.06.004> (2013).
- Makawita, S. & Tawbi, H. A. Nonsurgical Management of Melanoma Brain Metastasis: current therapeutics, challenges, and strategies for Progress. *Am. Soc. Clin. Oncol. Educ. Book.* **41**, 79–90. https://doi.org/10.1200/edbk_321137 (2021).
- Rulli, E., Legramandi, L., Salvati, L. & Mandala, M. The impact of targeted therapies and immunotherapy in melanoma brain metastases: a systematic review and meta-analysis. *Cancer.* **125**, 3776–3789. <https://doi.org/10.1002/cncr.32375> (2019).
- Zhou, S. et al. Role of the tumor microenvironment in malignant melanoma organoids during the development and metastasis of tumors. *Front. Cell. Dev. Biology.* **11** <https://doi.org/10.3389/fcell.2023.1166916> (2023).
- Kircher, D. A., Silvis, M. R., Cho, J. H. & Holmen, S. L. Melanoma Brain Metastasis: mechanisms, models, and Medicine. *Int. J. Mol. Sci.* **17** <https://doi.org/10.3390/ijms17091468> (2016).
- Hicks, W. H. et al. Contemporary Mouse Models in Glioma Research. *Cells.* **10** <https://doi.org/10.3390/cells10030712> (2021).
- Sachs, N. et al. A Living Biobank of Breast Cancer Organoids Captures Disease Heterogeneity. *Cell* **172**, 373–386. <https://doi.org/10.1016/j.cell.2017.11.010> (2018). <https://doi.org/10.1016/j.cell.2017.11.010>
- Pernik, M. N. et al. Patient-derived Cancer Organoids for Precision Oncology Treatment. *J. Pers. Med.* **11** <https://doi.org/10.3390/jpm11050423> (2021).
- Kim, M. et al. Patient-derived lung cancer organoids as in vitro cancer models for therapeutic screening. *Nat. Commun.* **10**, 3991. <https://doi.org/10.1038/s41467-019-11867-6> (2019).
- Abdullah, K. G. et al. Establishment of patient-derived organoid models of lower-grade glioma. *Neuro-oncology.* **24**, 612–623. <https://doi.org/10.1093/neuonc/noab273> (2022).
- Shi, D. D. et al. De novo pyrimidine synthesis is a targetable vulnerability in IDH mutant glioma. *Cancer cell.* **40**, 939–956. <https://doi.org/10.1016/j.ccell.2022.07.011> (2022).
- Vilgelm, A. E. et al. Fine-needle aspiration-based patient-derived Cancer Organoids. *iScience.* **23**, 101408. <https://doi.org/10.1016/j.isci.2020.101408> (2020).
- Phifer, C. J. et al. Obtaining patient-derived cancer organoid cultures via fine-needle aspiration. *STAR. Protocols.* **2**, 100220. <https://doi.org/10.1016/j.xpro.2020.100220> (2021). <https://doi.org/https://doi.org/>
- Zheng, S. et al. SynergyFinder Plus: toward Better Interpretation and Annotation of Drug Combination Screening datasets. *Genom. Proteom. Bioinform.* **20**, 587–596. <https://doi.org/10.1016/j.gpb.2022.01.004> (2022).
- Buehler, J. D. et al. Semi-automated computational Assessment of Cancer Organoid viability using Rapid Live-Cell Microscopy. *Cancer Inf.* **21**, 11769351221100754. <https://doi.org/10.1177/11769351221100754> (2022).
- Willis, B. C., Johnson, G., Wang, J. & Cohen, C. SOX10: a useful marker for identifying metastatic melanoma in sentinel lymph nodes. *Appl. Immunohistochem. Mol. Morphol.* **23**, 109–112. <https://doi.org/10.1097/pai.000000000000097> (2015).
- Keung, E. Z. & Gershenwald, J. E. The eighth edition American Joint Committee on Cancer (AJCC) melanoma staging system: implications for melanoma treatment and care. *Expert Rev. Anticancer Ther.* **18**, 775–784. <https://doi.org/10.1080/14737140.2018.1489246> (2018).
- Shannan, B., Perego, M., Somasundaram, R. & Herlyn, M. Heterogeneity in Melanoma. *Cancer Treat. Res.* **167**, 1–15. https://doi.org/10.1007/978-3-319-22539-5_1 (2016).
- Gregg, R. K. in *In Melanoma: Methods and Protocols.* 1–21 (eds Hargadon, K. M.) (Springer US, 2021).
- Yu, S. et al. A modified nucleoside 6-Thio-2'-Deoxyguanosine exhibits Antitumor Activity in Gliomas. *Clin. cancer Research: Official J. Am. Association Cancer Res.* **27**, 6800–6814. <https://doi.org/10.1158/1078-0432.Ccr-21-0374> (2021).
- Wei, S. et al. Antitumor Activity of a mitochondrial-targeted HSP90 inhibitor in Gliomas. *Clin. cancer Research: Official J. Am. Association Cancer Res.* **28**, 2180–2195. <https://doi.org/10.1158/1078-0432.Ccr-21-0833> (2022).
- Zhuang, L. et al. Activation of the extracellular signal regulated kinase (ERK) pathway in human melanoma. *J. Clin. Pathol.* **58**, 1163–1169. <https://doi.org/10.1136/jcp.2005.025957> (2005).
- Haass, N. K. et al. The mitogen-activated protein/extracellular signal-regulated kinase kinase inhibitor AZD6244 (ARRY-142886) induces growth arrest in melanoma cells and tumor regression when combined with docetaxel. *Clin. cancer Research: Official J. Am. Association Cancer Res.* **14**, 230–239. <https://doi.org/10.1158/1078-0432.Ccr-07-1440> (2008).
- Bollag, G. et al. Clinical efficacy of a RAF inhibitor needs broad target blockade in BRAF-mutant melanoma. *Nature.* **467**, 596–599. <https://doi.org/10.1038/nature09454> (2010).
- Ji, S. et al. Pharmaco-proteogenomic characterization of liver cancer organoids for precision oncology. *Sci. Transl. Med.* **15**, eadg3358. <https://doi.org/10.1126/scitranslmed.adg3358> (2023).
- van de Wetering, M. et al. Prospective derivation of a living Organoid Biobank of Colorectal Cancer patients. *Cell.* **161**, 933–945. <https://doi.org/10.1016/j.cell.2015.03.053> (2015). <https://doi.org/https://doi.org/>
- Hicks, W. H. et al. Creation and development of patient-derived organoids for therapeutic screening in Solid Cancer. *Curr. Stem Cell Rep.* **8**, 107–117. <https://doi.org/10.1007/s40778-022-00211-2> (2022).

34. Chen, C. C. et al. Patient-derived tumor organoids as a platform of precision treatment for malignant brain tumors. *Sci. Rep.* **12**, 16399. <https://doi.org/10.1038/s41598-022-20487-y> (2022).
35. Jacob, F. et al. A Patient-Derived Glioblastoma Organoid Model and Biobank Recapitulates Inter- and Intra-tumoral Heterogeneity. *Cell* **180**, 188–204 e122 (2020). <https://doi.org/10.1016/j.cell.2019.11.036>
36. Ou, L. et al. Patient-derived melanoma organoid models facilitate the assessment of immunotherapies. *EBioMedicine*. **92**, 104614. <https://doi.org/10.1016/j.ebiom.2023.104614> (2023).
37. El Shami, M. et al. Human plasma-like medium facilitates metabolic tracing and enables upregulation of immune signaling pathways in glioblastoma explants. *bioRxiv*. <https://doi.org/10.1101/2023.05.29.542774> (2023).

Author contributions

Conceptualization: KGA, SKM, WHH; Methodology: WHH, KGA; Investigation: WHH, LCG, MES, TER; Formal Analysis: WHH, LCG, MES, TER; Writing – Original Draft: WHH, KGA; Writing – Review & Editing: WHH, JIT, DD, YGN, LCG, SKM, and KGA; Visualization: WHH, LCG, MES; Supervision: KGA, SKM; Funding Acquisition: KGA.

This project was supported by NIH grant P30CA047904 awarded to UPMC Hillman Cancer Center.

Declarations

Competing interests

The authors declare no competing interests.

Ethical Statement

All patient tissue and blood samples were collected following ethical and technical guidelines on the use of human samples for biomedical research at the University of Pittsburgh after informed consent was obtained from patients under the Institutional Review Board Protocol (19080321). The study was conducted according to the principles of the Declaration of Helsinki.

Consent to participate and publish

Informed written consent was obtained from all individual participants included in this study. The authors affirm that human research participants provided informed consent for the publication of the images in Figs. 2 and 3.

Additional information

Correspondence and requests for materials should be addressed to K.G.A.

Reprints and permissions information is available at www.nature.com/reprints.

Publisher's note Springer Nature remains neutral with regard to jurisdictional claims in published maps and institutional affiliations.

Open Access This article is licensed under a Creative Commons Attribution-NonCommercial-NoDerivatives 4.0 International License, which permits any non-commercial use, sharing, distribution and reproduction in any medium or format, as long as you give appropriate credit to the original author(s) and the source, provide a link to the Creative Commons licence, and indicate if you modified the licensed material. You do not have permission under this licence to share adapted material derived from this article or parts of it. The images or other third party material in this article are included in the article's Creative Commons licence, unless indicated otherwise in a credit line to the material. If material is not included in the article's Creative Commons licence and your intended use is not permitted by statutory regulation or exceeds the permitted use, you will need to obtain permission directly from the copyright holder. To view a copy of this licence, visit <http://creativecommons.org/licenses/by-nc-nd/4.0/>.

© The Author(s) 2024